ELSEVIER

Ceramics International 31 (2005) 945–951

CERAMICS INTERNATIONAL

www.elsevier.com/locate/ceramint

Influence of cobalt phase on mechanical properties and thermal shock performance of Al_2O_3–TiC composites

Jing Li [a], Lai-peng Ma [b,*]

[a] *Department of Materials Science and Engineering, Shandong Institute of Architecture and Engineering, Jinan 250101, PR China*
[b] *Key Laboratory of Material Liquid Structure and Heredity of Education Ministry-Key Laboratory of Engineering Ceramics, Shandong University, Jinan 250061, PR China*

Received 11 May 2004; received in revised form 1 September 2004; accepted 10 October 2004
Available online 8 March 2005

Abstract

Cobalt phase was introduced into Al_2O_3–TiC composites to improve resistance to thermal shock by hot pressing cobalt coated powders. The thermal shock properties of the composites were evaluated by water quenching method and compared with the traditional Al_2O_3–TiC composites. The composites containing only 4 vol.% cobalt exhibited higher critical temperature difference (ΔT_c) and retained tensile strength. The calculation of thermal shock parameters (R parameters) indicates that the incorporation of cobalt improves the resistance to crack initiation and propagation under thermal shock, which should be attributed to enhanced tensile strength, fracture toughness and thermal conductivity as well as decreased Young's modulus. Noticeable improvement in crack deflection, bridging and blunting caused by cobalt phase are responsible for the increased crack stability in terms of the change in microstructure. The presence of cobalt in the matrix was also found to inhibit the oxidation of TiC.

Keywords: C. Mechanical properties; C. Thermal shock resistance; D. Al_2O_3

1. Introduction

Al_2O_3–TiC (AT) composites have been widely used in various engineering fields with its high strength, hardness, chemical stability and excellent wear resistance relative to Al_2O_3 ceramics [1,2]. In many applications the Al_2O_3–TiC composites are often exposed to rapid temperature changes that might cause severe thermal stress and thermal shock damage. High-strength dense ceramics, high resistance to thermal shock is especially required. However, they possess low thermal shock resistance due to their lower fracture toughness, thermal conductivity, etc. Therefore, thermal shock resistance is a major issue in their structural applications.

It has been known that the incorporation of secondary phases (whiskers, fibers, and metallic particles) into a ceramic matrix can bring about improvement on mechanical properties, including thermal shock performance. Among these methods, metallic particle toughened ceramic–matrix composites are promising candidates for high temperature applications having a superior crack growth resistance when compared with monolithic ceramics, as well as excellent high temperature strength when compared with metallic alloys. The toughening mechanisms should be mainly attributed to the improvement of mechanical behavior (crack blunting, shielding and crack deflection accompanied by particle pull out) and physical properties (e.g. thermal conductivity, Young's modulus) [3–13]. Nevertheless, the incorporation of large amount of metallic phase in the form of particle, usually exhibiting poor wettability to the ceramic matrix, resulted in serious metal agglomeration and then formation of large voids, limiting the exertion of toughening effects [3–9]. The powder coating technique has proved to be an effective method in processing ceramic–matrix composites, which was found to greatly improve the homogeneity,

* Corresponding author. Tel.: +86 531 8392439; fax: +86 531 8392439.
E-mail address: aahans@hotmail.com (L. Ma).

0272-8842/$30.00
doi:10.1016/j.ceramint.2004.10.007

Table 1
Thermo-mechanical properties of components at room temperature

Properties	Cobalt	Al_2O_3	TiC
Thermal conductivity (W/m K)	100	20	24
Young's modulus (GPa)	209	380	450
Thermal expansion ($\times 10^{-6}$ K^{-1})	14.2	8.5	7.6
Poisson ratio	0.31	0.22	0.17

sinterability and interfacial reliability with relatively small amount of metallic phase [14,15]. Cobalt, a common cohesive phase in cermets, possesses favorable wettability to TiC, which is expected to improve the interfacial reliability and then mechanical properties. Comparing with Al_2O_3 and TiC, cobalt possesses a unique set of physical properties (see Table 1), e.g. higher thermal conductivity and lower Young's modulus, which should make it very suitable for increasing the thermal shock resistance of Al_2O_3–TiC composites [2,10–12,16]. In the present work, therefore, we prepared a sort of novel Al_2O_3–TiC–Co composites (ATC) from cobalt-coated ceramic powders that was obtained by a newly developed coating technique, which was expected to improve the mechanical and thermal shock performance.

The thermal shock behavior of ATC composites was evaluated by water quenching technique and subsequent three point bending tests of tensile strength. Parallel reference experiments were conducted with dense Al_2O_3–TiC composites. In order to assess specifically the effects of cobalt phase on thermal shock behavior, four thermal shock parameters (R parameters) were introduced for both composites in terms of their mechanical and physical properties. Moreover, the relationship between thermal shock behavior and microstructure of ATC composites was investigated by means of the SEM micrographs of fracture surfaces.

2. Experimental

The Al_2O_3 (average particle size ~70 nm) and TiC (average particle size ~130 nm) powders were coated with Cobalt film, respectively. The coated powders with the weight ratio of 7:3 (Al_2O_3:TiC) (provided by the copartners of Zhejiang University, China) were then homogenized by conventional ball-milling as the starting powders. The coated powders were hot-pressed in vacuum at 1650 °C for 30 min, under a pressure of 30 MPa. For comparison, Al_2O_3–TiC composites were prepared at 1700 °C for 30 min under 30 MPa. The hot-pressed bodies were cut into bars (3 mm × 4 mm × 36 mm), ground and polished to 1 μm finish before fracture strength testing. And the specimen edges were slightly beveled on 1200-grit emery paper to remove notches introduced in the course of machining. The test bars were heated to desired temperatures for 30 min in a drop-bottom furnace and then quenched into a container of water at 25 °C. The thermal quenching of single thermal shock was conducted at initial temperatures ranging from 25 to 1025 °C, which corresponded to thermal shock temperature differences of 0–1000 °C. Repeated thermal shock tests, up to 20 cycles, were carried out at $\Delta T = 400$ °C.

Five samples were tested for each temperature difference. The shocked bars were dried before their retained strength was measured at room temperature. The tensile strength of specimens was determined by three point bending tests, with a span length of 20 mm and a crosshead speed of 0.5 mm/min. The fracture toughness (K_{IC}) was measured by the single-edge notch beam (SENB, the notch width: 0.22 mm and the depth: 2 mm) method. Thermal conductivity was measured using a laser flash thermo-conductive technique and thermal expansion was determined experimentally using a push-rod dilatometer at room temperature. Young's modulus was determined using the standard equation [17]:

$$E = \frac{L^3 m}{4WD^3} \tag{1}$$

where L is the length of support span, W is the specimen width, D is the specimen thickness, and m is the slope of the tangent of the initial straight-line portion of the load–deflection curve. Modulus values were calculated by drawing a tangent to the steepest initial straight-line portion of the load–deflection curve using Eq. (1). For the simplicity of the calculation, the values of the Poisson ratio (μ) for both composites were assumed to be identical, and this assumption, for the ATC composites with only 4 vol.% cobalt addition, is basically reasonable. Generally, for the composites reinforced by particles, the Poisson ratio of composites can be estimated from [18]:

$$\mu_c = \mu_m V_m + \mu_p V_p \tag{2}$$

where V is the volume fraction, m and p represent matrix and reinforced particles, respectively. In this system, μ_m and μ_p are taken to be 0.22 and 0.17, respectively [19].

Average grain size was determined from intercept measurements on the SEM images of thermal etched surfaces, by using the standard equation [20]:

$$\bar{D} = 1.56\bar{L} \tag{3}$$

where $\bar{D}$ is the average grain size and $\bar{L}$ is the average intercept length. At least 100 grains were counted in each specimen. The densities of the sintered samples were measured using Archimedes principle, and the theoretical density was calculated from the law of mixtures. The phase composition after thermal shock was identified on the fracture surface using X-ray diffraction (XRD) (D/max-rA, Japan) with Cu Kα radiation. The fracture surfaces were investigated using a scanning electron microscope (SEM) (Hitachi S-2500) equipped with an EDX system for elemental analysis (Link–ISIS300 Oxford).

Table 2
Component and mechanical properties of the ATC and AT composites

	Al_2O_3 (vol.%)	TiC	Co	Relative density (%)	Average grain size (μm)	Flexural strength (MPa)	Fracture toughness (MP $m^{1/2}$)
ATC	71	25	4	99.2	2.8	782 ± 60	7.8 ± 0.8
AT	74	26	/	99.6	3.1	559 ± 41	4.9 ± 0.3

3. Results and discussion

Table 2 summarizes the components and mechanical properties of ATC and AT composites. The relative density of ATC composite was slightly lower than the AT composite, which may be due to some voids caused by the presence of cobalt particles [5,7,8]. For the ATC composite, the average grain size was also smaller than that of the AT, revealing that the cobalt particles act as grain boundary pinning for matrix grain growth [5–8,10,21]. The incorporation of 4 vol.% cobalt phase that acted as inhibitors for grain growth, markedly affected the strength. The tensile strengths for the ATC and AT composite were measured to be 782 ± 60 and 559 ± 41 MPa, respectively. The fracture toughness for the ATC exhibited 7.8 ± 0.8 MPa $m^{1/2}$, which was increased by 60% in comparison to 4.9 ± 0.3 MPa $m^{1/2}$ of AT composites. Fig. 1 shows the typical SEM micrographs of the fracture surfaces of the ATC composites. EDS analysis reveals that the cobalt phase is characterized by small bright particles. The cobalt phase is distributed uniformly in the matrix, mostly located at the grain boundaries and partly within the grains, exhibiting the intra-and intergranular type. It could be clearly seen that there are many small cobalt particles (sub-micron size) and corresponding voids left by particle pullout. EDS results also indicates that the interfaces between Al_2O_3 and TiC grains are occupied by cobalt phase, which may be the result of the favorable wettability between cobalt and TiC.

It is well known that the thermal expansion mismatch led to residual compressive stress between TiC particles and Al_2O_3 matrix, which is considered to be the primary toughening mechanism of Al_2O_3–TiC composites [1]. Cracks have been observed in the fracture surface of ATC composite, where TiC particles play an effective role in crack branching, bridging and deflection. The fracture surfaces show a large proportion of transgranular cracks with some intergranular type, unlike the intergranular fracture mode of traditional Al_2O_3–TiC composites. It is suggested that cobalt phase enhances interfacial bonding, leading to the change of fracture mode. Previous works [22,23] showed that when intersecting a large TiC particle part of the cracks propagated directly through the TiC particles with a little or without deflection. No crack bridging was observed in the vicinity of the TiC particles. These phenomena were assumed to be the result of the brittleness of TiC particles. However, these could be rarely found in the ATC composites. It is reasonably concluded that crack tip was effectively blunted by the ductile cobalt phase located at the TiC/Al_2O_3 interface when it came across to the TiC particles. The high compressive stress developed around cobalt particles could also constrain the propagation of a crack whose plane contains the particle and deflect the crack away, thereby increasing the resistance of crack propagation. As a result, additional energy would be needed to initiate a new crack path and thus the resistance to further crack extension is enhanced [7,8,10]. Therefore, higher values of fracture toughness should be attributed to more effective energy consuming mechanisms in the ATC composite.

Fig. 2 shows the effects of single thermal shock on the tensile strength of AT and ATC composites. The strength behavior of both materials follows Hasselman's theory [33] that predicts a discontinuity with considerable strength degradation at a critical thermal shock temperature difference ΔT_c. The retained tensile strength of both composites decreased moderately within a certain shock ΔT and then sharply dropped at a point corresponding to the ΔT_c, followed by a gradual decrease for further increasing temperature difference. The curve for AT composite presented the usual drop of tensile strength for a critical ΔT_c of about 250 °C. With further increase in ΔT, the retained strength decreased gradually from 125 to 16 MPa. The ATC composite, however, exhibited a greater resistance

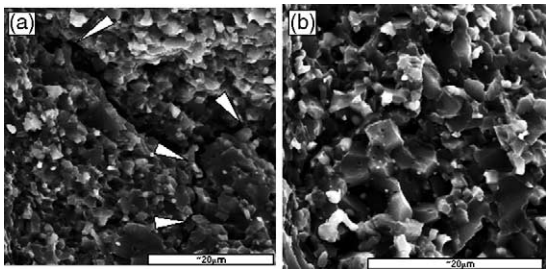

Fig. 1. SEM micrographs of the fracture surface of ATC composites.

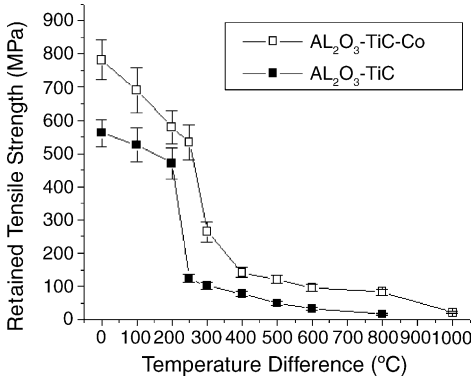

Fig. 2. Dependence of retained tensile strength on thermal shock temperature difference for the ATC and AT composites.

to crack initiation and crack propagation, possessing increased ΔT_c (about 350 °C) and, higher retained strength (from 264 to 83 MPa) up to 800 °C. The effect of cobalt phase is evident: its incorporation into Al_2O_3–TiC matrix through the powder coating technique improves the mechanical properties and the thermal shock resistance.

The thermal shock resistance of brittle materials depends on a series of properties: tensile strength, fracture toughness, thermal conductivity, Young's modulus, thermal expansion coefficient, etc. [10–13,20,24–31]. Several thermal shock parameters (R parameters) have been defined to relate these thermo-physical and thermo-mechanical properties of the materials to their thermal shock resistance, considering the crack initiation and crack propagation conditions, respectively. The most used ones are defined as [32,33]:

$$R = \frac{\sigma(1-\mu)}{\alpha E} \tag{4}$$

$$R' = \frac{k\sigma(1-\mu)}{\alpha E} \tag{5}$$

$$R''' = \frac{K_{IC}^2}{\sigma^2(1-\mu)} \tag{6}$$

$$R_{st} = \left(\frac{\gamma_f}{\alpha^2 E}\right)^{1/2} \tag{7}$$

where k is the thermal conductivity, σ the tensile strength, μ the Poisson ratio, α the coefficient of thermal expansion, E the Young's modulus of elasticity, K_{IC} the fracture toughness and γ_f the surface fracture energy. Generally, these properties, especially thermal conductivity, exhibit significant dependence on temperature. Nevertheless, it is expected the results of thermal shock test would show a positive correlation with the various thermal shock resistance parameters calculated from the room temperature data.

R and R' parameters predict the critical temperature difference (ΔT_c) in a body under conditions of sharp and moderate heat flow, respectively, which are expressed as the resistance to crack initiation [32]. Based on Eqs. (4) and (5), destruction of materials by thermal shock is determined by the thermal stress generated during severe thermal quenching. A material with higher thermal conductivity, tensile strength and lower Young's modulus, Poisson ratio and coefficient of thermal expansion, in general, possesses a better resistance to thermal shock owing to its tendency to reduce interior temperature differences and thermal stress. As shown in Table 2, the tensile strength was increased about 40% for ATC composite in comparison with AT composite. Tensile strength appears to be predominant in determining R. In the case of ATC composite, the reinforcing effects of cobalt phase should be responsible for it. Al_2O_3 and TiC are both typical dielectric solid with lower values of k [20]. The incorporation of cobalt (λ = 100 W/m K) was expected to increase the thermal conductivity of the matrix. Likewise, the presence of cobalt phase (E = 209 GPa) would decrease the Young's modulus of the composites [20]. Experimental data in Table 3 confirm this trend. For the ATC composite containing 4 vol.% Co, the measured thermal conductivity is 21.8 W/m K that is improved by around 6%. Young's modulus decreases from 391 ± 27 to 377 ± 30 GPa. It may be concluded that the powder coating technique adopted in this work promoted the uniform distribution of the cobalt phase, which resulted in effective increase in thermal conductivity and reduction in stiffness, relative to the traditional ball milling of the mixed powders. As shown in Table 3, the calculated values of R show that the ATC composite possesses a higher ΔT_c than that of the AT composite, with an increase of 52 °C. However, the result is lower than the experimental cure. This difference may be associated with the deviation of room temperature data adopted here. Compared with R, there is a greater increase in R' with the improved thermal conductivity.

Table 3
Mechanical and thermal properties of ATC and AT composites at room temperature

	Al_2O_3–TiC–Co	Al_2O_3–TiC
E (GPa)	377 ± 30	391 ± 27
ν	0.21	0.21
α ($\times 10^{-6}$ K^{-1})	8.36 ± 0.1	8.2 ± 0.1
k (W/m K)	21.8	20.6
γ_f (J/m^2)	80.9 ± 12.9	30.7 ± 4.6
R (°C)	193	141
R' (W/m)	4212.5	2904.6
R''' ($\times 10^{-6}$)	99	53
R_{st} (m$^{1/2}$ K$^{1/2}$)	1.73 ± 0.14	1.07 ± 0.08

R''' and R_{st} parameter express the ability of a material to resist crack propagation and further damage and loss of strength with increasing severity of thermal shock [33]. Higher R''' and R_{st} values indicate higher retained strength and crack stability once the critical temperature drop ΔT_c is exceeded. In order to improve R''' and R_{st}, high K_{IC}, γ_f and relatively low σ values are demanded on the basis of Eqs. (6) and (7). In this work, there is an increase of 60% in fracture toughness for ATC with only 40% increase in tensile strength. Although the tensile strength of ATC is obviously enhanced, higher fracture toughness seems to be predominant in determining R'''. Table 3 indicates that the ATC composite exhibited 87% improvements in R''' with the presence of cobalt phase. Likewise, R_{st} increases around 64% because of higher effective surface energy (80.9 ± 12.9) that increases by a factor of 2.64. It could be concluded on this basis that the ATC composites possess greater resistance to crack propagation and to further thermal shock damage than the AT composites. In fact, the relationship between retained tensile strength and original strength, namely, the resistance to thermal shock damage, could be described as [26]:

$$\frac{\sigma_r}{\sigma_o} \sim R''' \sim \frac{\gamma_{WOF}}{\gamma_{ic}} \tag{8}$$

where σ_r is the retained tensile strength, σ_o the strength before thermal shock, γ_{WOF} the work of fracture, and γ_{ic} the fracture surface energy. According to Eq. (8), the retained

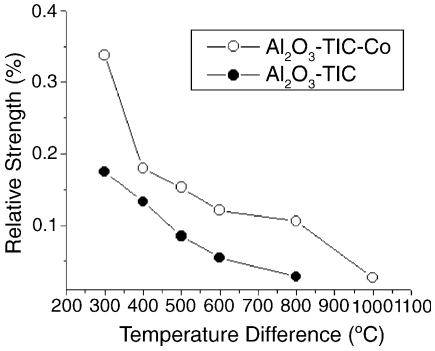

Fig. 3. Dependence of relative strength on thermal shock temperature difference for the ATC and AT composites.

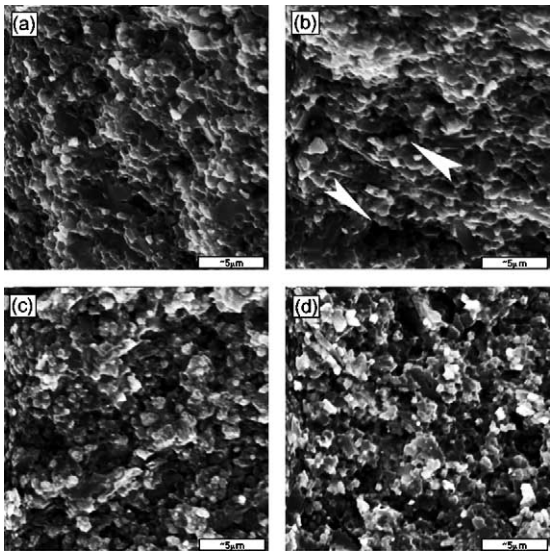

Fig. 4. SEM images of the fracture surface of ATC composites after thermal shock (ΔT) at: (a) 400 °C, (b) 600 °C, (c) 800 °C, and (d) 1000 °C.

tensile strength ratio is directly proportional to R''''. It can be then predicted on this basis that 4 vol.% Cobalt would provide a significant improvement in retained strength through increased difficulty of crack propagation, as a result of the increased fracture toughness. As mentioned above, the presence of the cobalt phase could, to some extent, promote the crack bridging and crack deflection effects of TiC particles. Furthermore, the ductile cobalt phase at the interface between TiC and Al_2O_3 particles was assumed to take effect in restraining crack propagation by crack tip blunting, serving as an effective energy consuming mechanisms. Fig. 3 confirms that the trends in the R'''' are consistent with measurements of thermal shock damage with increasing temperature drop (from $\Delta T = 300$ to 800 °C). Especially when ΔT increased from 600 to 800 °C, the retained strength of ATC remained almost constant, while that of the AT composite dropped suddenly to 3% ($\Delta T = 800$ °C) of its original strength. However, when ΔT was up to 1000 °C, there was a sharp drop of retained strength from 14 to 2.7%. As shown in Fig. 4, when ΔT is below 600 °C, the grain boundaries are clear and fracture mode is mixture of transgranular and intergranular type. But there were few isolated voids after thermal shock, which may be ascribed to the thermal stresses in the body. As ΔT reaches 800 °C, more and larger voids were found and the isolated voids turned to interpenetrating ones. And the fracture surface exhibited trace of oxidation, which was identified as Co_3O_4 by the XRD pattern. But it was not found that the oxidation of TiC occurred by XRD. With further increase to $\Delta T = 1000$ °C, intergranular fracture turns to be the primary fracture mode and the oxidation seems to be more serious together with pronounced voids interpenetration, as shown in Fig. 4(d). XRD pattern (Fig. 5) confirms that TiO_2 (rutile) forms after thermal shock at this temperature difference, which is usually found in Al_2O_3–TiC after heat treatment at $\Delta T = 800$ °C [34]. It is clear that the formation of large numbers of TiO_2 and corresponding voids decrease the grain boundary bonding and brought the sharp drop in retained strength of ATC composite at $\Delta T = 1000$ °C. On the other hand, however, the cobalt phase and corresponding oxide on the interfaces could inhibit, to a degree, the oxidation reaction of TiC at relatively high temperature, which is expressed as follows [34]:

$$TiC + 2O_2 = TiO_2 + CO_2 \uparrow$$

The dependence of strength on thermal shock cycles for both composites quenched at $\Delta T = 400$ °C is given in Fig. 6. The change in strength as a function of the cumulative number of thermal shock cycles is presumably because of the accumulation and coalescence of thermal-shock-induced microcracks and voids damage. The strength of both materials decreased initially rapidly and then tended to

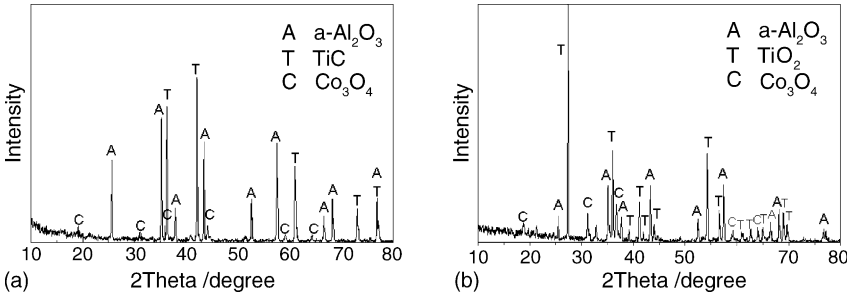

Fig. 5. XRD of ATC composites after thermal shock (ΔT) at: (a) 800 °C and (b) 1000 °C.

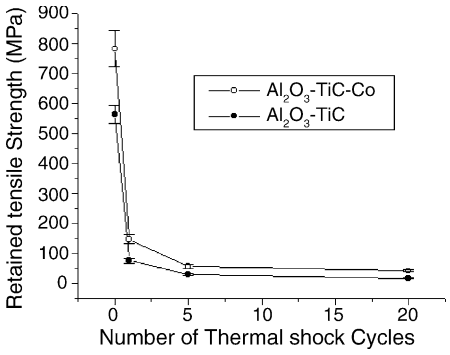

Fig. 6. Dependence of retained strength on thermal shock cycles ($\Delta T = 400\ ^{\circ}C$).

saturation values with increasing number of thermal shock cycles. Likewise, the higher retained strength was also obtained in ATC composites, suggesting that the ATC composite is less sensitive to repeated thermal shock than the AT composite at such temperature drop. After one thermal shock cycle, ATC possessed 18% of its original strength while AT had only 14%. With increasing thermal shock number above five times, the retained strength of ATC remained almost constant (about 7%), AT decreasing relatively rapidly to 2.3%. Such damage of AT composites could be induced by stresses arising from expansion mismatch between Al_2O_3 and TiC particles, thermal expansion anisotropy of the Al_2O_3 grains and stresses from the non-linear temperature distribution present during the quenching in water. As for ATC composites, the ductile cobalt phase between Al_2O_3 and TiC particles is assumed to relieve the thermal stresses to a degree, which should be responsible for the higher resistance to thermal shock damage. Further observation was carried out on the fracture surface of ATC composites to investigate the damage mechanisms. After five times of thermal shock cycles, larger and interpenetrating voids were seen and the fracture surface exhibited few orchid-like products of oxidation that could be universally found after twenty cycles (Fig. 7). EDS results confirm that it is also the oxide of Titanium, which is concluded to be TiO_2 (rutile) according to previous study

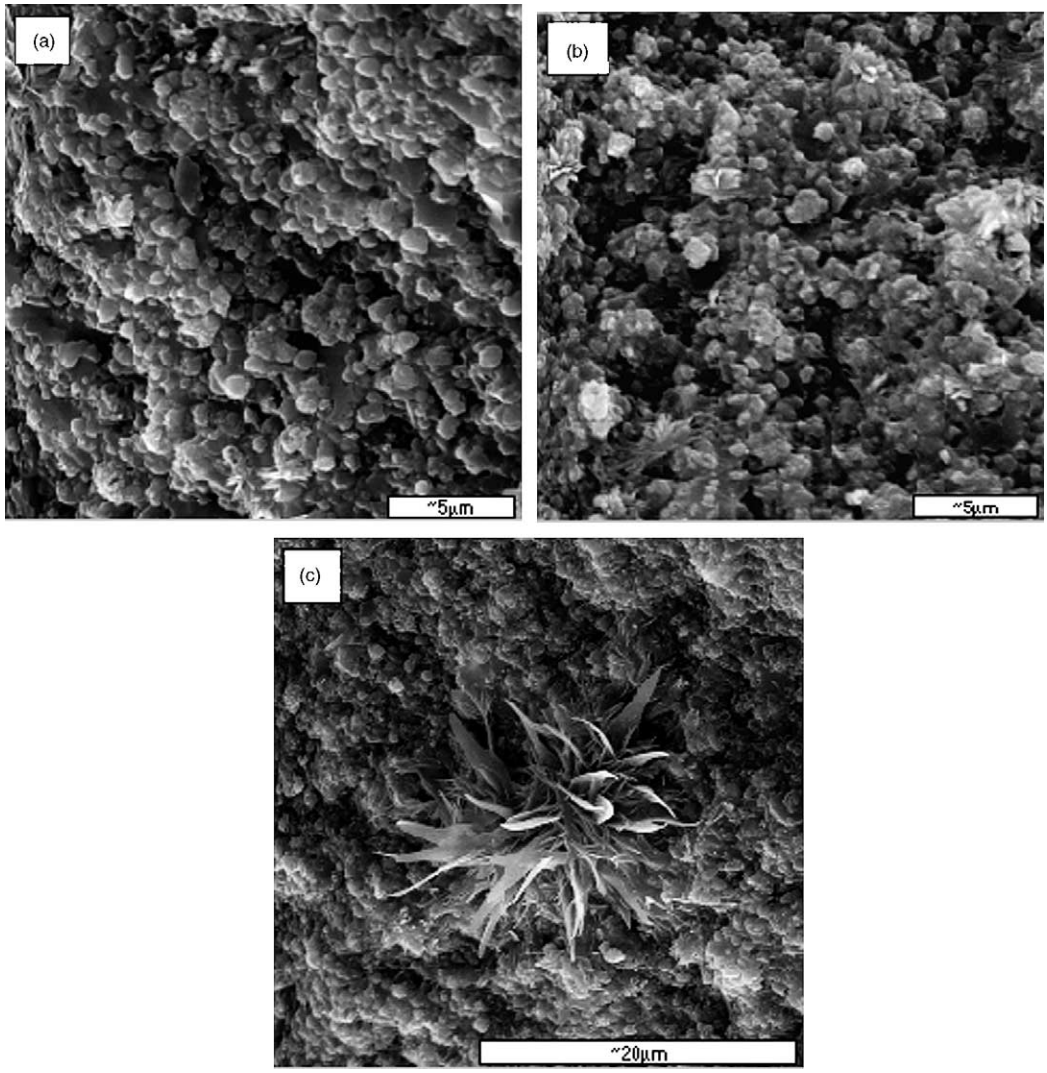

Fig. 7. SEM micrographs of the fracture surface of ATC composites after thermal shock cycles ($\Delta T = 400\ ^{\circ}C$) (a), 5 times (b), and (c) 20 times.

[34]. It appears that the bonding and toughening effects of cobalt phase decreased sharply with increasing cycles, the presence of oxide and voids impairing the continuity of the body severely. At last, the formation of interpenetrating voids and TiO_2 leads to the serious degradation of the ATC composites.

4. Conclusions

The novel Al_2O_3–TiC–Co composites with only 4 vol.% cobalt inclusion showed better thermal shock resistance than the traditional Al_2O_3–TiC composites. Water quenching experiment indicated that the incorporation of cobalt provide beneficial contribution to both the resistance to thermal shock fracture and thermal shock damage. The improvement in thermal shock behavior by cobalt inclusions could be specifically explained by corresponding R parameters. The critical temperature difference for the ATC composites (∼350 °C) was improved about 100 °C compared with that of the AT composites (∼250 °C). This should be attributed to the enhanced strength and thermal conductivity but also lower Young's modulus, leading to higher R and R'. With increasing temperature difference, the retained strength of ATC composites was also improved, which was the result of enhanced R'''' and R_{st} with higher toughness and effective surface energy as well as relatively lower tensile strength. SEM micrographs of the fracture surfaces of the ATC composites revealed that cobalt phase promoted the crack branching, bridging and deflection effects, which result in the toughness increment. Crack blunting caused by the ductile cobalt phase was assumed to be also responsible for the enhanced stability of crack propagation under single and repeated thermal shock. As a whole, the presence of cobalt not only improves the thermal physical properties but also inhibits, to a degree, the oxidation of TiC.

Acknowledgement

This study was sponsored by the National "863" Program of China (Grant no. 2002A332100).

References

[1] R.P. Whai, B. Ilschner, J. Mater. Sci. 15 (1980) 875–885.
[2] J. Zhao, X. Ai, X.P. Huang, J. Mater. Process. Tech. 129 (2002) 161–166.
[3] Y.-J. Lin, B.-F. Jiang, J. Am. Ceram. Soc. 81 (9) (1998) 2481–2484.
[4] W.-P. Tai, T. Watanabe, J. Am. Ceram. Soc. 81 (1) (1998) 257–259.
[5] T. Sekino, T. Nakajima, J. Am. Ceram. Soc. 80 (5) (1997) 1139–1148.
[6] S.-T. Oh, M. Sando, K. Nihara, J. Am. Ceram. Soc. 81 (11) (1998) 3013–3015.
[7] J. Lu, L. Gao, J. Sun, L. Gui, J. Guo, Mater. Sci. Eng. A 293 (2000) 223–228.
[8] J. Lu, L. Gao, J. Sun, Mater. Chem. Phys. 72 (2001) 352–355.
[9] W.-P. Tai, Y.-S. Kim, J.-G. Kim, Mater. Chem. Phys. 82 (2003) 396–400.
[10] O. Sbaizero, G. Pezzotti, Mater. Sci. Eng. A 343 (2003) 273–281.
[11] L. Wang, J.L. Shi, M.T. Lin, H.R. Chen, Mater. Res. Bull. 36 (2001) 925–932.
[12] L. Wang, J.L. Shi, J.H. Gao, D.S. Yan, J. Eur. Ceram. Soc. 21 (2001) 1213–1217.
[13] A.A. Khan, J.C. Labbe, Mater. Sci. Eng. A 230 (1997) 33–38.
[14] T.D. Mitchell Jr., L.C. De Jonghe, J. Am. Ceram. Soc. 78 (1995) 199.
[15] D. Vollath, D.V. Szabo, J. Haubelt, J. Eur. Ceram. Soc. 17 (1997) 1317.
[16] N. Chawlaa, B.V. Patelb, M. Koopmanb, Mater. Character. 49 (2003) 395–407.
[17] ASTM D790M-86, Standard Test Methods for Flexural Properties of Unreinforced and Reinforced Plastics and Electrical Insulating Materials, Annual Book of ASTM Standards, vol. 08.01. ASTM, 1988, pp. 290–298.
[18] A.A. Fahmy, A.N. Ragai, J. Appl. Phys. 13 (1970) 5108–5111.
[19] I. Pollini, A. Mosser, J.C. Parlebas, Phys. Rep. 355 (2001) 1–72.
[20] S.C. Cooper, P.T.A. Hodson, Trans. J. Br. Ceram. Soc. 81 (1982) 121.
[21] M. Hamidouche, N. Bouaouadja, C. Olagnon, Ceram. Int. 29 (2003) 599–609.
[22] J. Gong, Z. Zhao, H. Miao, Scripta Mater. 43 (2000) 27–31.
[23] J. Gong, H. Miao, Z. Zhao, J. Eur. Ceram. Soc. 21 (2001) 2377–2381.
[24] C. Aksel, Ceram. Int. 29 (2003) 183–188.
[25] C. Aksel, F.L. Riley, J. Eur. Ceram. Soc. 23 (2003) 3079–3087.
[26] A.F. Emery, in: D.P.H. Hasselman, R.A. Heiler (Eds.), Thermal Stresses in Severe Environment, Plenum Press, New York, 1980, pp. 95–121.
[27] Y.C. Ko, Ceram. Int. 27 (2001) 501–507.
[28] P. Pettersson, M. Johnsson, J. Eur. Ceram. Soc. 23 (2003) 309–313.
[29] P. Pettersson, Z. Shen, M. Johnsson, M. Nygren, J. Eur. Ceram. Soc. 22 (2002) 1357–1365.
[30] R.J. Damani, D. Rubesa, R. Danzer, J. Eur. Ceram. Soc. 20 (2000) 1439–1452.
[31] S. Maensiri, S.G. Roberts, J. Eur. Ceram. Soc. 22 (2002) 2945–2956.
[32] W.D. Kingery, J. Am. Ceram. Soc. 38 (3) (1955) 3–15.
[33] D.P.H. Hasselman, J. Am. Ceram. Soc. 52 (11) (1969) 600–604.
[34] L. Zhang, R.V. Koka, Mater. Chem. Phys. 57 (1998) 23–32.